Biochem. J. (2012) **447**, 353–361 (Printed in Great Britain) doi:10.1042/BJ20120750

Farnesyl diphosphate synthase, the target for nitrogen-containing bisphosphonate drugs, is a peroxisomal enzyme in the model system *Dictyostelium discoideum*

James M. NUTTALL, Ewald H. HETTEMA[1] and Donald J. WATTS[1]

Department of Molecular Biology and Biotechnology, University of Sheffield, Firth Court, Western Bank, Sheffield S10 2TN, U.K.

NBP (nitrogen-containing bisphosphonate) drugs protect against excessive osteoclast-mediated bone resorption. After binding to bone mineral, they are taken up selectively by the osteoclasts and inhibit the essential enzyme FDPS (farnesyl diphosphate synthase). NBPs inhibit also growth of amoebae of *Dictyostelium discoideum* in which their target is again FDPS. A fusion protein between FDPS and GFP (green fluorescent protein) was found, in *D. discoideum*, to localize to peroxisomes and to confer resistance to the NBP alendronate. GFP was also directed to peroxisomes by a fragment of FDPS comprising amino acids 1–22. This contains a sequence of nine amino acids that closely resembles the nonapeptide PTS2 (peroxisomal targeting signal type 2): there is only a single amino acid mismatch between the two sequences. Mutation analysis confirmed that the atypical PTS2 directs FDPS into peroxisomes. Furthermore, expression of the *D. discoideum* FDPS–GFP fusion protein in strains of *Saccharomyces cerevisiae* defective in peroxisomal protein import demonstrated that import of FDPS into peroxisomes was blocked in a strain lacking the PTS2-dependent import pathway. The peroxisomal location of FDPS in *D. discoideum* indicates that NBPs have to cross the peroxisomal membrane before they can bind to their target.

Key words: *Dictyostelium discoideum*, farnesyl diphosphate synthase, mevalonate pathway, nitrogen-containing bisphosphonate drugs, peroxisomal targeting signal, peroxisome.

INTRODUCTION

The mevalonate pathway of isoprenoid biosynthesis allows eukaryotic cells to convert acetyl-CoA into FDP (farnesyl diphosphate). FDP is mainly used for biosynthesis of sterols but it may also be used, either directly or after conversion into geranylgeranyl diphosphate, for protein prenylation [1]. The mevalonate pathway also provides precursors for synthesis of dolichol, the isoprenoid side-chain of ubiquinone, the side-chain of haem A and for prenylation of tRNA species. In plants, FDP derived from this pathway is also the precursor for biosynthesis of sesquiterpenes and triterpenes [2,3].

The mevalonate pathway was originally considered to be cytosolic, but the first indications that this might not be correct came in 1994 when investigations making use of antibodies to detect either mevalonate kinase or FDPS (FDP synthase) in mammalian cells indicated that both of these enzymes are peroxisomal [4,5]. Furthermore, it was found that there was decreased activity of the mevalonate pathway enzymes in tissue from patients suffering from peroxisome-deficiency diseases (e.g. Zellweger's syndrome) and this appeared to imply a peroxisomal location for all of the pathway enzymes [5]. Although later studies of knockout mouse models for Zellweger's syndrome have since cast doubt on the conclusion that peroxisome deficiency leads to low activity of the mevalonate pathway enzymes [6,7], further immunocytochemical investigations appeared to confirm that the pathway enzymes are peroxisomal (reviewed in [8]), except for 3-hydroxy-3-methylglutaryl-CoA reductase which is associated with the endoplasmic reticulum [9]. However, subsequent investigations (reviewed in [10]) have failed to confirm the proposed peroxisomal localization for the pathway enzymes in mammalian cells, and it has been concluded that the enzymes are cytosolic [10]. Hence, at present, the intracellular location of the mammalian mevalonate pathway enzymes remains unclear. The pathway has also been investigated in plants and it appears that some, but not all, of the enzymes are peroxisomal, and that there may also be mitochondrial isoenzymes of both isopentenyl diphosphate isomerase and FDPS [3,11–13]. However, synthesis of FDP in plants is complex because, in addition to the mevalonate pathway, there is a second pathway for FDP biosynthesis [14].

Peroxisomal enzymes are post-translationally imported into the peroxisomal matrix. Most contain an evolutionarily conserved PTS (peroxisome targeting signal) 1 at their extreme C-terminus that is a tripeptide consisting of Ser-Lys-Leu or variants derived from this sequence [15]. A few use a PTS2 comprising a non-apeptide with the consensus sequence (R/K)(L/I/V/Q)XX(L/I/V/H/Q)(L/S/G/A/K)X(L/A/F) (where X can be any amino acid) found near the N-terminus [16]. The PTS1 and PTS2 are recognized by the cytosolic import receptors Pex5p and Pex7p respectively. These receptors deliver their cargo to the docking complex on the peroxisomal membrane and then participate in the translocation of the cargo across the peroxisomal membrane [17].

Some peroxisomal matrix proteins possess neither a PTS1 nor a PTS2. Such proteins may be imported after binding Pex5p, despite lacking a PTS1 (e.g. *Saccharomyces cerevisiae* acyl-CoA oxidase [18]) or by a process termed 'piggybacking' involving association with other proteins possessing a PTS sequence. The latter process has been demonstrated for the co-import of mammalian SOD (superoxide dismutase), which lacks a PTS, with the copper chaperone of SOD1 which possesses a PTS1 [19] and, in experimental conditions, for several homomultimeric proteins (e.g. *S. cerevisiae* peroxisomal 3-oxoacyl-CoA thiolase [20]).

Abbreviations used: FDP, farnesyl diphosphate; FDPS, FDP synthase; *Dd*FDPS, *Dictyostelium discoideum* FDPS; GFP, green fluorescent protein; HcRed, *Heteractis crispa* red fluorescent protein; mRFP, monomeric red fluorescent protein; NBP, nitrogen-containing bisphosphonate; PTS, peroxisome targeting signal; RFP, red fluorescent protein; SOD, superoxide dismutase.

[1] Correspondence may be addressed to either of these authors (email e.hettema@sheffield.ac.uk or d.j.watts@sheffield.ac.uk).

The intracellular location of FDPS is of particular interest because this enzyme is the target for an important group of drugs, the NBPs (nitrogen-containing bisphosphonates). These drugs specifically inhibit bone resorption by osteoclasts and are therefore used to treat conditions in which bone resorption is excessive (e.g. Paget's disease, tumoral bone disease and osteoporosis) [21]. Two of the NBPs (alendronate and risedronate) are so widely prescribed, especially for treatment of osteoporosis, that they fall into the category of 'blockbuster' drugs.

Although the therapeutic use of the NBPs is to inhibit osteoclast-mediated bone resorption, the drugs are also able to inhibit growth of amoebae of the cellular slime mould *Dictyostelium discoideum* and it was owing to use of *D. discoideum* as a model system that it was first proved that FDPS is the target for the drugs [22,23]. A sequence of nine amino acids (Arg-Ala-Ala-Met-Ile-Ser-Glu-His-Leu) near the N-terminal end of *Dd*FDPS (*Dictyostelium discoideum* FDPS) is closely related to the PTS2 consensus sequence. Furthermore, in *Dictyostelium purpureum* and *Dictyostelium fasciculatum* the corresponding sequence is totally in accordance with the PTS2 consensus sequence (Figure 1A). Investigations were therefore designed to test whether the putative PTS2 in *Dd*FDPS does direct the protein to peroxisomes.

EXPERIMENTAL

Dictyostelium plasmids

Oligonucleotides used in the present study are shown in Table 1. A DNA fragment encoding GFP (green fluorescent protein) S65T was ligated between the BamHI and Xba1 sites in pDXA3C [24] to give pGFP. Similarly, pGFP–PTS1 was obtained by ligation of a BamHI–XbaI fragment encoding GFP plus the C-terminal PTS1 sequence Pro-Leu-His-Ser-Lys-Leu from pEH012 [25] into pDXA3C.

The oligonucleotide (FDP 1 coding) that encodes the N-terminal 22 amino acids of *Dd*FDPS plus the amino acid linker sequence Gly-Ala-Gly and oligonucleotide (FDP 1 non-coding) were annealed and then ligated into HindIII- and BamHI-digested pGFP1 to give p1-22–GFP.

The DNA fragment amplified from pLD1A15SN [26] by use of primers VIP 660 and VIP 661 encoded FDPS with the addition of the C-terminal sequence Gly-Ala-Gly-Ala. This DNA fragment was digested with HindIII and BamHI and ligated into HindIII- and BamHI-digested pGFP to give pFDPS–GFP.

Oligonucleotides VIP 566 and VIP 567 were annealed and ligated into BamHI- and ClaI-digested p339-3mRFPmars [27] to give pmRFP–PTS1 that encodes mRFP (monomeric red fluorescent protein) with the additional C-terminal PTS1-containing sequence Pro-Leu-His-Ser-Lys-Leu. Similarly, oligonucleotides VIP 570 and VIP 571 were used, together with BamHI- and ClaI-digested p339-3mRFPmars, to give pmRFP encoding mRFP with the C-terminal sequence Pro-Thr-Asn-Thr-Ile-His-Arg.

A version of pFDPS–GFP, encoding only amino acids 11–382 of FDPS fused to GFP [pFDPS–GFP-(Δ1–10)], was obtained by using oligonucleotides VIP 712 and VIP 661 to allow amplification of the appropriate part of pLD1A15SN. The DNA fragment was digested with HindIII and BamHI and ligated between the HindIII and BamHI sites in pGFP. Oligonucleotides VIP 712 and VIP 767 were used in amplification of a DNA fragment from p1-22–GFP that was digested with HindIII and XbaI and ligated into p1-22–GFP that had also been digested with HindIII and XbaI. This gave a version (p11-22–GFP) of p1-22–GFP encoding only amino acids 11–22 of FDPS fused to GFP.

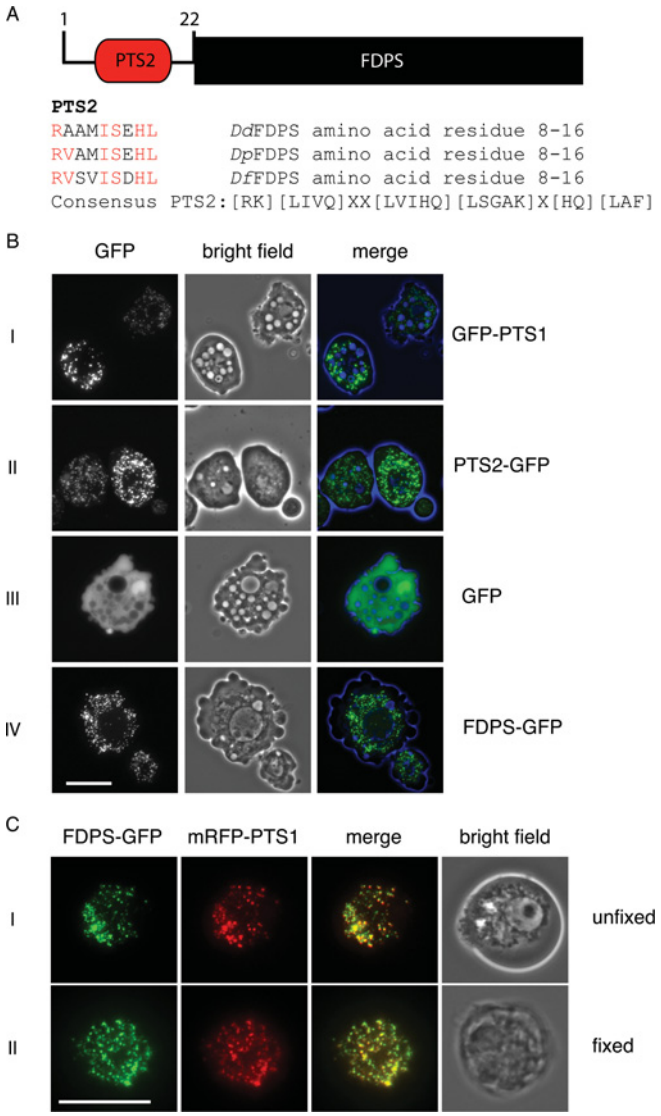

Figure 1 ***Dd*** **FDPS localizes to peroxisomes**

(**A**) Schematic representation of *Dd*FDPS showing the putative PTS2 in red. The amino acid sequence of the PTS2 in FDPS from *D. discoideum* (UniProt number Q9NH03) is compared with the amino acid sequences of the consensus PTS2 sequences in FDPS from the related species *D. purpureum* (*Dp*) (UniProt number F0Z8Y9) and *D. fasciculatum* (*Df*) (UniProt number F4PYV9). Amino acid residues matching the consensus sequence are indicated in red. The consensus PTS2 sequence is shown in the form proposed in [16]. (**B**) Amoebae expressing GFP–PTS1 (I), *S. cerevisiae* thiolase (possessing a PTS2) fused to GFP (PTS2–GFP) (II), GFP (III) or *Dd*FDPS–GFP (IV) were imaged by use of epifluorescence microscopy and the images are shown as maximum intensity projections of *Z*-stacks. (**C**) Unfixed amoebae expressing both mRFP–PTS1 and FDPS–GFP were imaged (I). Because peroxisomes tend to move during imaging, the RFP and GFP fluorescence do not appear to colocalize completely. However, after amoebae had been fixed in 3.6% (v/v) formaldehyde (II), complete colocalization of the RFP and GFP fluorescence is apparent, although fixation partially destroys cell morphology. 'Merge' is the overlay of the GFP fluorescence and the bright-field image (**B**) or the overlay of the GFP and RFP fluorescence (**C**). Scale bar represents 20 μm.

A HindIII site was introduced by PCR in front of the open reading frame encoding *S. cerevisiae* thiolase fused to GFP (a gift from S.J. Gould) [28] by using oligonucleotide VIP 1029 and the M13 reverse primer. The product was digested with HindIII and EcoRI and the fragment of approximately 600 bp was isolated. The fragment obtained by PCR was also digested with EcoRI and XbaI and the fragment of approximately 1400 bp was recovered. The 600 and 1400 bp fragments were ligated simultaneously into p1-22–GFP that had been digested with HindIII and XbaI to give

Table 1 Oligonucleotides used in the present study

Oligonucleotide	Sequence (5′→3′)
FDP 1 coding	AGCTTAAAAAATGAACAACCAATCACTCCAAAGAGCTGCTATGATATCTGAACACTTAGCTCCAACTTCAGAA TTAGGTGCTGGTG
FDP 1 non-coding	GATCCACCAGCACCTAATTCTGAAGTTGGAGCTAAGGTTCAGATATCATAGCAGCTCTTGGACTGATTGGTTGTTCATTTTTTA
VIP 566	GATCCCCATTACATTCAAAATTATAAGAATTCAT
VIP 567	CGATGAATTCTTATAATTTTGAATGTAATGGG
VIP 570	GATCCCCAACAAATACAATTCATAGATAAGAATTCAT
VIP 571	CGATGAATTCTTATCTATGAATTGTATTTGTTGGG
VIP 660	GACAAGCTTAAAAAAATGAACAACCAATCACTC
VIP 661	GCAGGATCCAGCACCAGCACCTAAATCTCTTTTATAAATCTTT
VIP 712	GACAAGC TTAA AAAATGATATCTGAACACTTAGC
VIP 740	GAGCTGCTATGATATCTGAAGCCTTAGCTCCAACTTCAG
VIP 741	CTGAAGTTGGAGCTAAGGCTTCAGATATCATAGCAGCTC
VIP 767	GATCCTCTAGACTAAGATC
VIP 898	GAACAACCAATCACTCC AAGCTGCTGCTATGATATCTGAAC
VIP 899	GTTCAGATATCATAGCAG CAGCTTGGAGTGATTGGTTGTTC
VIP 1029	GACAAGCTTAAAAAATGTCTCAAAGACTACAAAGTATC

pPTS2–GFP. This strategy was used to avoid the HindIII site in the EcoRI–XbaI fragment. All constructs were sequenced to confirm the nucleotide sequences.

Growth and transformation of *D. discoideum*

Amoebae of *D. discoideum* strain Ax-2 were grown at 22 °C in HL5 glucose medium with shaking at 160 rev./min [29]. Amoebae were transformed by electroporation [30] with two pulses of 0.65 kV at 25 Ω. Transformants were selected by addition of the appropriate antibiotic (G418 at 10 μg/ml or Blasticidin S at 10 μg/ml) to the growth medium.

Site-directed mutagenesis

A Stratagene QuikChange® Site-Directed Mutagenesis kit was used according to the manufacturer's instructions. Oligonucleotides VIP 898 and VIP 899 were used to prime replication of p1-22–GFP or pFDPS–GFP. In each of the resulting plasmids [p1-22–GFP (R8A) and pFDPS–GFP (R8A) respectively], the initial arginine residue in the putative PTS2 sequence had been replaced by an alanine residue.

To produce plasmids in which the histidine residue in the putative PTS2 sequence had been replaced by an alanine residue, oligonucleotides VIP 740 and VIP 741 were employed in replication of pFDPS–GFP and p1-22–GFP to produce pFDPS–GFP (H15A) and p1-22–GFP (H15A) respectively.

Yeast strains, medium and growth conditions

The *S. cerevisiae* strains used were BY4742, BY4742 *pex5*::kanMX and BY4742 *pex7*::kanMX (Euroscarf). Cells were grown overnight in defined selective glucose medium [2 % (w/v) glucose, 0.17 % yeast nitrogen base and 0.5 % ammonium sulfate]. For analysis of phenotypes by microscopy, cells were subsequently diluted to a D_{600} of 0.1 in fresh selective glucose medium and grown for two to three cell divisions (4–6 h) before imaging. The appropriate amino acid stocks were added to minimal medium as required.

Yeast plasmids

Yeast *Dd*FDPS expression plasmids were based on the parental plasmids ycplac33 and ycplac111 [31] containing the *TPI1* promoter region and *PGK1* terminator. The constructs used in the present study were generated by homologous recombination in yeast [32]. The *Dd*FDPS open reading frame in pFDPS–GFP was amplified by PCR. The 5′ ends of the primers included 18 nucleotide extensions, homologous with plasmid sequences flanking the intended insertion site, to enable repair of gapped plasmids by homologous recombination. The HcRed (*Heteractis crispa* RFP)–PTS1 expression plasmid has been described previously [25].

Digitonin

Approximately 1.5×10^6 amoebae were washed twice with 1.0 ml of 0.7 % NaCl containing 20 mM K_2HPO_4/KH_2PO_4 (pH 7.0) and resuspended in 100 μl of buffered saline containing 5 μg of digitonin (Sigma).

Image acquisition

Unfixed cells were analysed with an Axiovert 200M microscope (Carl Zeiss) equipped with an Exfo X-cite 120 excitation light source, appropriate band-pass filters (Carl Zeiss and Chroma), a Neofluar 40×/1.3 NA (numerical aperture) Oil Ph3 objective lens (Carl Zeiss) and a digital camera (Orca ER, Hamamatsu). Image acquisition was performed by use of Volocity software (PerkinElmer). Fluorescence images were routinely collected as 1 μm *Z*-stacks which were merged into one plane and processed further in Photoshop (Adobe) where only the level adjustment was used. On occasion (as indicated in the text) a single plane of the *Z*-stack was used. Bright-field images were collected in one plane.

RESULTS

*Dd*FDPS is a peroxisomal enzyme

When GFP appended with Ser-Lys-Leu (GFP–PTS1) was expressed in *D. discoideum* amoebae, its fluorescence showed a punctate pattern typical for peroxisomes containing GFP (Figure 1B). By contrast, fluorescence of unmodified GFP was seen throughout the cytosol (Figure 1B). As a reporter for the PTS2 import pathway we used *S. cerevisiae* 3-oxoacyl-CoA thiolase, which possesses a consensus PTS2 fused to GFP. A typical peroxisomal pattern of fluorescence was observed (Figure 1B). These observations are in agreement with previous reports that both the PTS1 and PTS2 protein import pathways operate in *D. discoideum* [33–35].

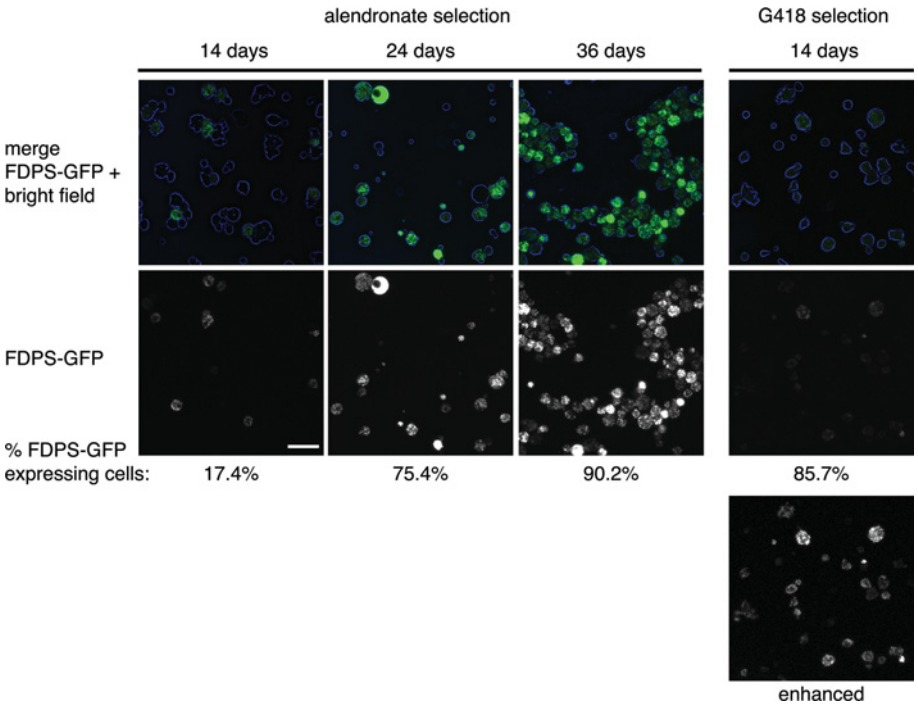

Figure 2 FDPS–GFP expression in *D. discoideum* amoebae gives rise to resistance to alendronate

Amoebae were transformed with the *Dd*FDPS–GFP expression plasmid (pFDPS–GFP) and grown in the presence of either alendronate (80 μM) or the antibiotic G418 (10 μg/ml). Amoebae were imaged by use of epifluorescence microscopy at the times indicated after addition of either alendronate or G418. All images were captured with the same exposure times and processed identically. An enhanced image of G418-selected cells is included to show the high percentage of low-expressing cells. The percentage of cells displaying detectable FDPS–GFP expression is indicated for each time point (at least 200 cells were counted each time). Scale bar represents 50 μm.

*Dd*FDPS lacks a PTS1 signal, but contains a putative PTS2 sequence near its N-terminus (Figure 1A). To investigate the intracellular localization of *Dd*FDPS, we tagged it at its C-terminus with GFP and expressed it in amoebae. A punctate pattern of fluorescence was observed (Figure 1B). In amoebae co-expressing FDPS–GFP and mRFP–PTS1 the patterns of GFP and mRFP fluorescence completely overlapped when the amoebae had been fixed before imaging (Figure 1C). We conclude that FDPS–GFP is localized to peroxisomes in *D. discoideum*.

When *D. discoideum* amoebae have increased activity of FDPS, owing to overproduction of this enzyme, their growth becomes resistant to inhibition by NBPs [23]. Similarly, amoebae overexpressing *Dd*FDPS–GFP were also found to be resistant to the effects of NBPs. The *Dd*FDPS–GFP expression plasmid also contained the neomycin-resistance gene encoding an aminoglycoside 3′-phosphotransferase which allows for selection of transformed cells with the antibiotic G418. Transformants, initially selected in G418-containing medium, were then able to grow in medium containing the NBP alendronate (160 μM). This concentration is at least 4-fold greater than the IC_{50} for inhibition of growth of untransformed amoebae by alendronate [36]. Furthermore, amoebae were transformed with the *Dd*FDPS–GFP expression plasmid and directly selected in medium containing 80 μM alendronate instead of G418. Since alendronate has primarily growth static effects [36], untransformed amoebae died only slowly but, over a period of 4 weeks, the proportion of *Dd*FDPS–GFP-expressing cells increased to over 90 % (Figure 2). In most of the cells, FDPS–GFP was expressed to a higher level than in the cells selected for G418 resistance (Figure 2) but the highly overexpressed FDPS–GFP was still confined to the peroxisomes. These results implied that FDPS–GFP is catalytically active within amoebae and, hence, that the FDPS is folded into its native three-dimensional conformation.

*Dd*FDPS–GFP is closely associated with peroxisomes

At low concentrations the detergent digitonin affects the permeability of the plasma membrane without having any detectable effects on the integrity of the peroxisomal membrane [37]. As a result, cytosolic proteins are released from cells during incubation with digitonin but there is no release of peroxisomal proteins. When amoebae co-expressing mRFP (used as a cytosolic marker protein) and *Dd*FDPS–GFP were treated with digitonin, the plasma membrane could be seen to disintegrate (Figure 3A, see bright-field panels), but only the mRFP was released from the amoebae. The fluorescence of *Dd*FDPS–GFP remained punctate within the amoebal ‘ghosts’ (Figure 3A).

Amoebae co-expressing mRFP–PTS1 and *Dd*FDPS–GFP were also incubated in digitonin. After the amoebae had lysed (Figure 3B, see bright-field panels), protein fluorescence indicated that *Dd*FDPS–GFP continued to co-localize with the peroxisomal marker protein mRFP–PTS1 (Figure 3B, see merged panels). We conclude that *Dd*FDPS–GFP is closely associated with peroxisomes.

*Dd*FDPS–GFP is imported into *S. cerevisiae* peroxisomes by use of the PTS2-dependent pathway

In *S. cerevisiae*, in contrast with most other organisms, the action of Pex7p (PTS2 receptor) is totally independent of the action of Pex5p, the PTS1 receptor [38]. We therefore used *S. cerevisiae* mutants to analyse genetically the association of

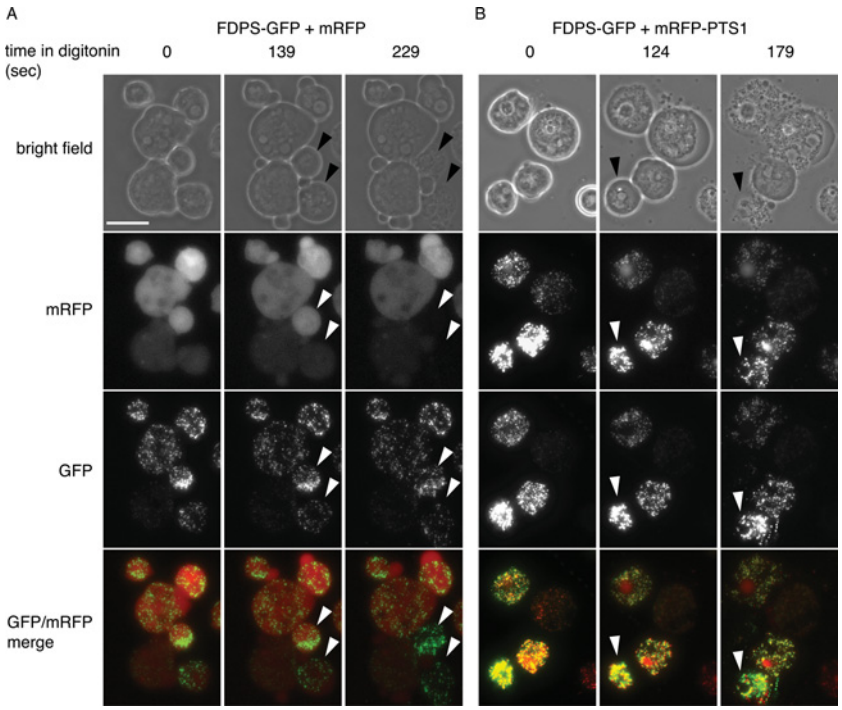

Figure 3 FDPS–GFP is closely associated with peroxisomes

Amoebae co-expressing *Dd*FDPS–GFP with either mRFP (**A**) or mRFP–PTS1 (**B**) were incubated with digitonin (50 μg/ml) and analysed by epifluorescence microscopy. Selective permeabilization of the plasma membrane at this digitonin concentration is slow and some cells permeabilize earlier than others. Arrowheads indicate cells with time-dependent permeabilization. Scale bar represents 20 μm.

FDPS with peroxisomes. *Dd*FDPS–GFP and HcRed–PTS1 were co-expressed in wild-type, *pex5Δ* and *pex7Δ S. cerevisiae* cells. *Dd*FDPS–GFP was imported into peroxisomes by wild-type cells, as indicated by co-localization with HcRed–PTS1 (Figure 4). However, targeting of *Dd*FDPS–GFP seemed less efficient than for the HcRed–PTS1 because some cytosolic background labelling could be observed. In *pex7Δ* cells, *Dd*FDPS–GFP no longer localized to the peroxisomes labelled with HcRed–PTS1, whereas in *pex5Δ* cells HcRed–PTS1 was mislocalized to the cytosol and *Dd*FDPS–GFP was localized to peroxisomes. These studies in *S. cerevisiae* indicate that *Dd*FDPS is imported into peroxisomes via the PTS2-dependent targeting pathway. All proteins that depend on either the PTS1 or the PTS2 pathway for their association with peroxisomes are matrix proteins because neither of these pathways is involved in import of peroxisomal membrane proteins [39]. Hence, the dependence of *Dd*FDPS import into peroxisomes on the PTS2 pathway indicates that *Dd*FDPS is a peroxisomal matrix protein.

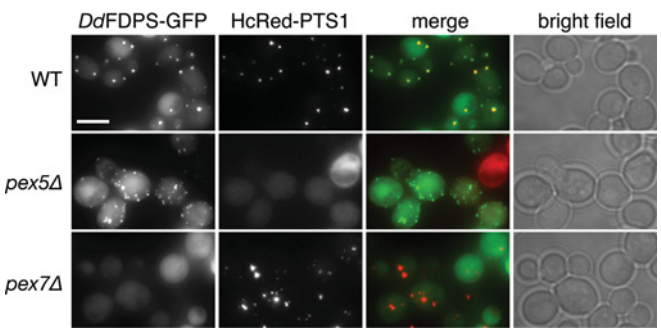

Figure 4 *Dd*FDPS–GFP is imported into *S. cerevisiae* peroxisomes via the PTS2 pathway

S. cerevisiae strains co-expressing the peroxisomal matrix marker HcRed–PTS1 and *Dd*FDPS–GFP were imaged by use of epifluorescence microscopy. Images are shown as maximum intensity projections of *Z*-stacks. Scale bar represents 5 μm. WT, wild-type.

*Dd*FDPS contains a PTS2

The presence of a putative PTS2 (amino acid residues 8–16) in *Dd*FDPS (Figure 1A) is consistent with the dependence of *Dd*FDPS–GFP import on Pex7p. To test whether the putative PTS2 of *Dd*FDPS is involved in peroxisomal import, we first fused an N-terminal fragment consisting of the first 22 amino acids of *Dd*FDPS to GFP and investigated its subcellular localization. It was found that this fusion protein localized to peroxisomes (1-22–GFP, Figure 5) and must therefore contain a functional targeting signal. In contrast, amino acids 11–22 of *Dd*FDPS fused at the N-terminal end to GFP (11-22–GFP) remained in the cytosol (Figure 5A). The PTS directing *Dd*FDPS into peroxisomes must therefore begin within the first ten N-terminal amino acids of the enzyme and the sequence comprising amino acids 8–16 could thus be the expected PTS2 sequence.

Site-directed mutagenesis was then used to confirm that residues 8–16 form the PTS2 by replacement of the two least variable residues (Arg^8 and His^{15}) in the consensus PTS2 by alanine. Replacement of the arginine residue by an alanine residue (R8A) in 1-22–GFP led to the fusion protein's accumulating in the cytosol instead of in the peroxisomes (Figure 5A). Subsitution of the histidine residue by alanine (H15A) in the putative PTS2 sequence partially impaired uptake into peroxisomes (Figure 5). These effects were similar to those found in previous investigations in which site-directed mutagenesis had been used

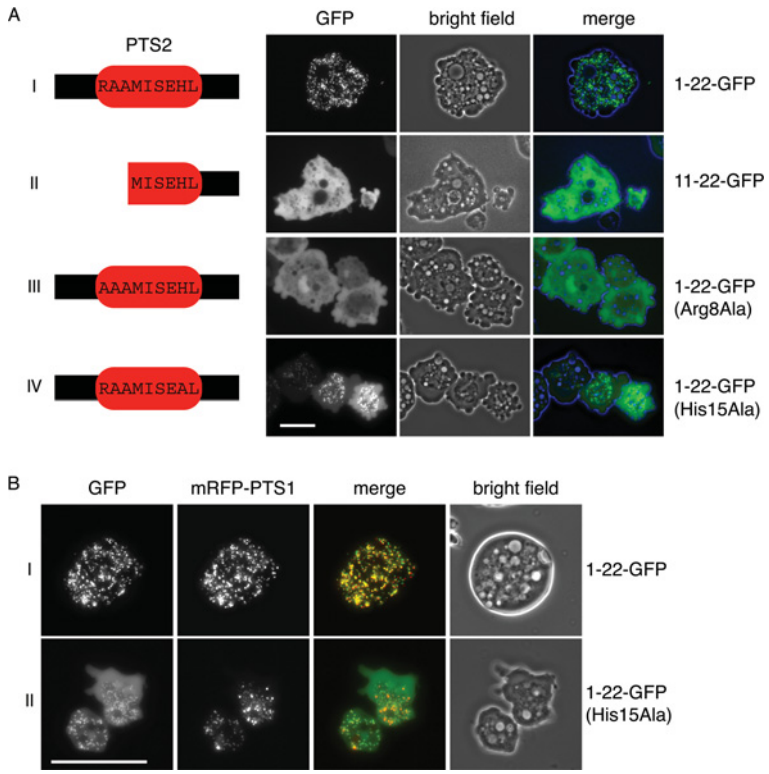

Figure 5 The N-terminus of *Dd*FDPS contains an atypical PTS2

(**A**) Characterization of the targeting information in the N-terminus of *Dd*FDPS. Amoebae were transformed to express either amino acid residues 1–22 (I) or amino acid residues 11–22 (II) of *Dd*FDPS fused to GFP. The first PTS2 amino acid residue (Arg^8) was mutated to alanine in the construct comprising amino acids 1–22 of *Dd*FDPS fused to GFP and expressed in *D. dicoideum* amoebae (III). Similarly, the eighth residue in the PTS2 (His^{15}) was also mutated to alanine (IV). Unfixed amoebae were imaged by epifluorescence microscopy and the images are shown as maximum intensity projections of *Z*-stacks. (**B**) Unfixed amoebae expressing mRFP–PTS1 and either 1-22–GFP (I) or 1-22–GFP (His15Ala) (II) were imaged. Scale bar represents 20 μm.

to replace either the arginine or histidine residues in the consensus PTS2 sequences of other peroxisomal enzymes [40,41]. The effects of site-directed mutagenesis were therefore entirely consistent with a conclusion that amino acids 8–16 in *Dd*FDPS form a functional PTS2 sequence, even though they comprise a sequence that differs slightly from that of the well-established consensus PTS2 sequence.

Effects of changes to the PTS2 sequence in the full-length amino acid sequence of *Dd*FDPS

The effects of destroying the PTS2 in the full-length *Dd*FDPS were subsequently investigated. A 10-amino-acid N-terminal truncation of FDPS–GFP was constructed that eliminated the initial part of the PTS2 and it was found that most of the fusion protein mislocalized to the cytosol, although some was still able to accumulate in peroxisomes (Figure 6). Similarly, the fusion protein comprising GFP linked to a mutant full-length version of *Dd*FDPS–GFP in which the PTS2 sequence was non-functional owing to replacement of the initial arginine residue with an alanine residue (R8A) accumulated in the cytosol, although some was able to localize to peroxisomes (Figure 6). The fusion protein between *Dd*FDPS containing the H15A mutation mainly mislocalized to the cytosol but some peroxisomal localization was also observed (Figure 6).

D. discoideum amoebae expressing fusion proteins comprising GFP linked to mutated forms of FDPS lacking a functional PTS2 sequence (i.e. having amino acids 1–10 deleted or containing the R8A mutation) were able to grow in 80 μM alendronate to

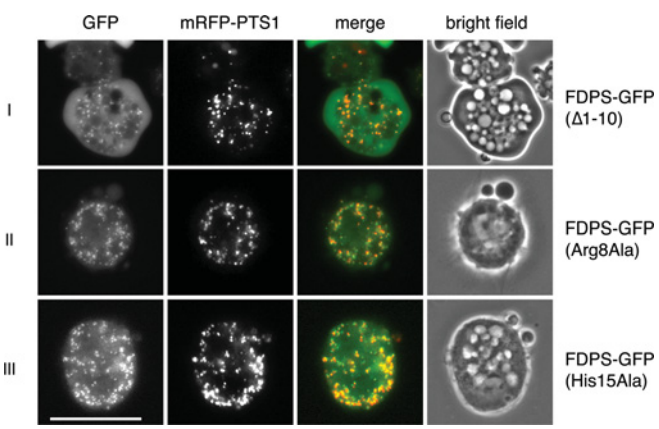

Figure 6 Peroxisomal import of *Dd*FDPS is only partially prevented by inactivation of the PTS2

Unfixed amoebae expressing both mRFP–PTS1 and mutant versions of FDPS–GFP were imaged, but only three consecutive slices from *Z*-stacks are shown as maximum intensity projections to allow the punctate GFP fluorescence to be seen more clearly. GFP fluorescence is present in both the cytosol and peroxisomes. Scale bar represents 20 μm.

the same final cell density as untransformed amoebae grown in the absence of alendronate. No growth could be detected for untransformed amoebae in 80 μM alendronate (results not shown). To confer this resistance to the growth-inhibitory effects of alendronate on amoebae, the mutant versions of FDPS–GFP must have been catalytically active, despite lacking a functional

PTS2 sequence, and, hence, must have been able to dimerize to form the active enzyme.

DISCUSSION

FDPS has been shown to be closely associated with the peroxisomes in *D. discoideum* by use both of fluorescence microscopy and selective permeabilization of the plasma membrane with digitonin. Close to the N-terminal end of the protein, there is a nonapeptide (amino acids 8–16) that, although not identical with the consensus PTS2 sequence, strongly resembles the consensus. Moreover, mutations in this sequence demonstrated that it behaves as a PTS2. Protein import into the peroxisomal matrix that is dependent on PTS2 requires recognition of the PTS2 by Pex7p and this protein was shown to be essential for the association of *Dd*FDPS with peroxisomes in *S. cerevisiae*. Hence it is concluded that *Dd*FDPS is a peroxisomal matrix protein.

The sequence in *Dd*FDPS that acts as the PTS2 is somewhat atypical because the second amino acid is alanine whereas the consensus PTS2 sequence contains a long-chain hydrophobic amino acid in this position (Figure 1A). This may be unique to FDPS in *D. discoideum* because inspection of the *D. discoideum* genome indicates that it does not seem to encode any other potential peroxisomal proteins containing the atypical PTS2. However, there is a medium-chain acyl-CoA oxidase in *Arabidopsis thaliana* that appears to have a PTS2 in which the second amino acid is also an alanine residue [42].

Although there is a functional PTS2 in *Dd*FDPS, it may appear that it is not essential for peroxisomal import of the enzyme because *Dd*FDPS–GFP, in which part of the PTS2 was either missing (i.e. amino acids 1–10 had been deleted) or non-functional (i.e. containing the R8A mutation), was still able to enter peroxisomes, albeit with low efficiency. This residual import could have been owing to a second signal downstream of the characterized PTS2 but the nature of any such signal is unclear.

The amoebae transformed with *Dd*FDPS–GFP fusion proteins lacking a functional PTS2 were able to grow in concentrations of alendronate that inhibited growth of untransformed amoebae. This indicated that these fusion proteins were catalytically active and, since *Dd*FDPS is a dimeric protein, that enzyme lacking a functional PTS2 is still able to form dimers. It is therefore possible that monomers of fusion proteins, apparently lacking a PTS2, dimerized with monomers of the endogenous *Dd*FDPS possessing a PTS2 to allow entry into peroxisomes by 'piggybacking'. The partial cytosolic accumulation of *Dd*FDPS–GFP lacking a PTS2 would then have resulted from formation of dimers between two *Dd*FDPS–GFP monomers both lacking a PTS2. This form of 'piggybacking' was previously demonstrated for the PTS2-containing protein thiolase from *S. cerevisiae*. When this enzyme, in which the PTS2 had been inactivated, was co-expressed with endogenous thiolase, it was found still to be imported into peroxisomes [20].

The exact means by which *Dd*FDPS that artificially lacks a PTS2 is able to enter peroxisomes could be of future interest but the phenomenon does not detract from the primary conclusion that *Dd*FDPS is a peroxisomal enzyme.

Although, thus far, it is only FDPS that has been shown to be a peroxisomal enzyme in *D. discoideum*, it would seem probable that other enzymes on the *D. discoideum* mevalonate pathway will also be found to be peroxisomal. Until these have been identified, it will not be possible to give a full description of the mevalonate pathway in *D. discoideum*. Furthermore, the pathway may also involve a number of previously unsuspected peroxisomal transport systems. The NBPs have to be able to cross the peroxismal membrane to reach and inhibit their target, *Dd*FDPS, and, since the NBPs carry three negative charges at physiological pH [43], it is improbable that passage through the peroxisomal membrane can be by simple diffusion. Entry on a transport system would appear more plausible and this proposal gains support from evidence that a transport system is required to transfer compounds containing negatively charged phosphate groups (AMP, ADP and ATP) across peroxisomal membranes [44,45]. A peroxisomal transport system mediating gratuitous transport of NBPs would most probably have one or more of the diphosphate intermediates on the mevalonate pathway as its natural ligand because the NBPs are analogues of some of these compounds (i.e. dimethylallyl diphosphate, isopentenyl diphosphate and geranyl diphosphate [23]). Clearly, complete understanding of the operation of the mevalonate pathway in *D. discoideum* will have to take into account not only the intracellular distribution of the pathway enzymes between the cytosol, peroxisomes and possibly the endoplasmic reticulum, but also the properties of any peroxisomal transport systems for the intermediates. NBPs have effects only on osteoclasts in patients taking the drugs to control bone disease but the intacellular location of the target, FDPS, in human cells is uncertain. It was first reported that human FDPS is peroxisomal [5] but later extensive investigations in mammalian cells [46] led to the conclusion that FDPS is cytosolic. More recently, an FDPS–GFP fusion protein was expressed in mammalian cells but it was not possible to determine whether it was located in the peroxisomes or in the cytosol [47]. The peroxisomal location of FDPS in *D. discoideum* does not necessarily imply that mammalian FDPS is also peroxisomal but there is a remarkable similarity between the rankings of NBPs in order of potency as inhibitors of bone resorption by mammalian osteoclasts and as inhibitors of growth of *D. discoideum* amoebae [36,48] and, in order to account for this, it would appear probable that mammalian FDPS resembles *Dd*FDPS in being peroxisomal. Furthermore, there may be only a limited correlation between the potency of NBPs as inhibitors of FDPS and as inhibitors of bone resorption [49,50], just as there is only a poor correlation between the potency of NBPs as inhibitors of *Dd*FDPS and as inhibitors of *D. discoideum* growth [23,43]. Such findings would arise if the effects of the NBPs on both bone resorption and *D. discoideum* growth are determined not only by their different potencies as inhibitors of FDPS but also by differences in their ability to cross the peroxisomal membrane.

Although investigations on *D. discoideum* have been limited to establishing the intracellular location for FDPS, they would imply that current understanding of the overall organization of the mevalonate pathway, and of the cellular events leading to inhibition of one of the pathway enzymes by the NBPs, is incomplete.

AUTHOR CONTRIBUTION

James Nuttall, Ewald Hettema and Donald Watts designed and performed the experiments and wrote the paper.

ACKOWLEDGEMENTS

We thank Dr R.R. Kay (MRC Laboratory of Molecular Biology, Cambridge, U.K.) for pDAXA3C, Dr A. Müller-Taubenberger (Institute for Cell Biology, Ludwig Maximilians University, Munich, Germany) for p339-3mRFPmars and Dr C.J. Sugden and Professor J.G. Williams (Wellcome Trust Biocentre, University of Dundee, Dundee, Scotland, U.K.) for pLD1A15SN. We are also grateful to Dr T. Abe (Wellcome Trust Biocentre, University of Dundee, Dundee, Scotland, U.K.) for advice about electroporation, to Dr A. Motley for assistance with fluorescence microscopy and to Victoria Motyer for generating the *Dd*FDPS–GFP yeast expression construct.

FUNDING

This work was supported, in part, by a Wellcome Trust Senior Research Fellowship [grant number WT 084265] to E.H.H.

REFERENCES

1 Goldstein, J. L. and Brown, M. S. (1990) Regulation of the mevalonate pathway. Nature **343**, 425–430
2 Tholl, D. (2006) Terpene synthases and the regulation, diversity and biological roles of terpene metabolism. Curr. Opin. Plant Biol. **9**, 297–304
3 Sapir-Mir, M., Mett, A., Belausov, E., Tal-Meshulam, S., Frydman, A., Gidoni, D. and Eyal, Y. (2008) Peroxisomal localization of *Arabidopsis* isopentenyl diphosphate isomerases suggests that part of the plant isoprenoid mevalonic acid pathway is compartmentalized to peroxisomes. Plant Physiol. **148**, 1219–1228
4 Biardi, L., Sreedhar, A., Zokaei, A., Vartak, N. B., Bozeat, R. L., Shackelford, J. E., Keller, G. A. and Krisans, S. K. (1994) Mevalonate kinase is predominantly localized in peroxisomes and is defective in patients with peroxisome deficiency disorders. J. Biol. Chem. **269**, 1197–1205
5 Krisans, S. K., Ericsson, J., Edwards, P. A. and Keller, G. A. (1994) Farnesyl-diphosphate synthase is localized in peroxisomes. J. Biol. Chem. **269**, 14165–14169
6 Hogenboom, S., Romeijn, G. J., Houten, S. M., Baes, M., Wanders, R. J. and Waterham, H. R. (2002) Absence of functional peroxisomes does not lead to deficiency of enzymes involved in cholesterol biosynthesis. J. Lipid Res. **43**, 90–98
7 Kovacs, W. J., Shackelford, J. E., Tape, K. N., Richards, M. J., Faust, P. L., Fliesler, S. J. and Krisans, S. K. (2004) Disturbed cholesterol homeostasis in a peroxisome-deficient PEX2 knockout mouse model. Mol. Cell. Biol. **24**, 1–13
8 Kovacs, W. J., Tape, K. N., Shackelford, J. E., Duan, X., Kasumov, T., Kelleher, J. K., Brunengraber, H. and Krisans, S. K. (2007) Localization of the pre-squalene segment of the isoprenoid biosynthetic pathway in mammalian peroxisomes. Histochem. Cell Biol. **127**, 273–290
9 Liscum, L., Finer-Moore, J., Stroud, R. M., Luskey, K. L., Brown, M. S. and Goldstein, J. L. (1985) Domain structure of 3-hydroxy-3-methylglutaryl coenzyme A reductase, a glycoprotein of the endoplasmic reticulum. J. Biol. Chem. **260**, 522–530
10 Wanders, R. J. and Waterham, H. R. (2006) Biochemistry of mammalian peroxisomes revisited. Annu. Rev. Biochem. **75**, 295–332
11 Simkin, A. J., Guirimand, G., Papon, N., Courdavault, V., Thabet, I., Ginis, O., Bouzid, S., Giglioli-Guivarc'h, N. and Clastre, M. (2011) Peroxisomal localisation of the final steps of the mevalonic acid pathway in planta. Planta **234**, 903–914
12 Thabet, I., Guirimand, G., Courdavault, V., Papon, N., Godet, S., Dutilleul, C., Bouzid, S., Giglioli-Guivarc'h, N., Clastre, M. and Simkin, A. J. (2011) The subcellular localization of periwinkle farnesyl diphosphate synthase provides insight into the role of peroxisome in isoprenoid biosynthesis. J. Plant Physiol. **168**, 2110–2116
13 Cunillera, N., Boronat, A. and Ferrer, A. (1997) The *Arabidopsis thaliana* FPS1 gene generates a novel mRNA that encodes a mitochondrial farnesyl-diphosphate synthase isoform. J. Biol. Chem. **272**, 15381–15388
14 Lichtenthaler, H. K. (1999) The 1-deoxy-D-xylulose-5-phosphate pathway of isoprenoid biosynthesis in plants. Annu. Rev. Plant Physiol. Plant Mol. Biol. **50**, 47–65
15 Gould, S. J., Keller, G. A. and Subramani, S. (1988) Identification of peroxisomal targeting signals located at the carboxy terminus of four peroxisomal proteins. J. Cell Biol. **107**, 897–905
16 Petriv, O. I., Tang, L., Titorenko, V. I. and Rachubinski, R. A. (2004) A new definition for the consensus sequence of the peroxisome targeting signal type 2. J. Mol. Biol. **341**, 119–134
17 Girzalsky, W., Saffian, D. and Erdmann, R. (2010) Peroxisomal protein translocation. Biochim. Biophys. Acta **1803**, 724–731
18 Klein, A. T., van den Berg, M., Bottger, G., Tabak, H. F. and Distel, B. (2002) *Saccharomyces cerevisiae* acyl-CoA oxidase follows a novel, non-PTS1, import pathway into peroxisomes that is dependent on Pex5p. J. Biol. Chem. **277**, 25011–25019
19 Islinger, M., Li, K. W., Seitz, J., Volkl, A. and Luers, G. H. (2009) Hitchhiking of Cu/Zn superoxide dismutase to peroxisomes: evidence for a natural piggyback import mechanism in mammals. Traffic **10**, 1711–1721
20 Glover, J. R., Andrews, D. W. and Rachubinski, R. A. (1994) *Saccharomyces cerevisiae* peroxisomal thiolase is imported as a dimer. Proc. Natl. Acad. Sci. U.S.A. **91**, 10541–10545
21 Fleisch, H. (1995) Bisphosphonates in Bone Disease. From the Laboratory to the Patient. The Parthenon Publishing Group, New York and London
22 Brown, R. J., Grove, J. E., Russell, R. G., Ebetino, F. H. and Watts, D. J. (1997) Bisphosphonate drugs inhibit farnesyl diphoshate synthase. Bone **20**, 115S
23 Grove, J. E., Brown, R. J. and Watts, D. J. (2000) The intracellular target for the antiresorptive aminobisphosphonate drugs in *Dictyostelium discoideum* is the enzyme farnesyl diphosphate synthase. J. Bone Miner. Res. **15**, 971–981
24 Manstein, D. J., Schuster, H. P., Morandini, P. and Hunt, D. M. (1995) Cloning vectors for the production of proteins in *Dictyostelium discoideum*. Gene **162**, 129–134
25 Motley, A. M. and Hettema, E. H. (2007) Yeast peroxisomes multiply by growth and division. J. Cell Biol. **178**, 399–410
26 Sugden, C. J., Roper, J. R. and Williams, J. G. (2005) Engineered gene over-expression as a method of drug target identification. Biochem. Biophys. Res. Commun. **334**, 555–560
27 Fischer, M., Haase, I., Simmeth, E., Gerisch, G. and Muller-Taubenberger, A. (2004) A brilliant monomeric red fluorescent protein to visualize cytoskeleton dynamics in *Dictyostelium*. FEBS Lett. **577**, 227–232
28 Kalish, J. E., Keller, G. A., Morrell, J. C., Mihalik, S. J., Smith, B., Cregg, J. M. and Gould, S. J. (1996) Characterization of a novel component of the peroxisomal protein import apparatus using fluorescent peroxisomal proteins. EMBO J. **15**, 3275–3285
29 Watts, D. J. and Ashworth, J. M. (1970) Growth of myxameobae of the cellular slime mould *Dictyostelium discoideum* in axenic culture. Biochem. J. **119**, 171–174
30 Pang, K. M., Lynes, M. A. and Knecht, D. A. (1999) Variables controlling the expression level of exogenous genes in *Dictyostelium*. Plasmid **41**, 187–197
31 Gietz, R. D. and Sugino, A. (1988) New yeast-*Escherichia coli* shuttle vectors constructed with *in vitro* mutagenized yeast genes lacking six-base pair restriction sites. Gene **74**, 527–534
32 Uetz, P., Giot, L., Cagney, G., Mansfield, T. A., Judson, R. S., Knight, J. R., Lockshon, D., Narayan, V., Srinivasan, M., Pochart, P. et al. (2000) A comprehensive analysis of protein-protein interactions in *Saccharomyces cerevisiae*. Nature **403**, 623–627
33 Fields, S. D., Arana, Q., Heuser, J. and Clarke, M. (2002) Mitochondrial membrane dynamics are altered in cluA- mutants of *Dictyostelium*. J. Muscle Res. Cell Motil. **23**, 829–838
34 Matsuoka, S., Saito, T., Kuwayama, H., Morita, N., Ochiai, H. and Maeda, M. (2003) MFE1, a member of the peroxisomal hydroxyacyl coenzyme A dehydrogenase family, affects fatty acid metabolism necessary for morphogenesis in *Dictyostelium* spp. Eukaryotic Cell **2**, 638–645
35 Huang, Y. C., Chen, Y. H., Lo, S. R., Liu, C. I., Wang, C. W. and Chang, W. T. (2004) Disruption of the peroxisomal citrate synthase CshA affects cell growth and multicellular development in *Dictyostelium discoideum*. Mol. Microbiol. **53**, 81–91
36 Rogers, M. J., Watts, D. J., Russell, R. G., Ji, X., Xiong, X., Blackburn, G. M., Bayless, A. V. and Ebetino, F. H. (1994) Inhibitory effects of bisphosphonates on growth of amoebae of the cellular slime mold *Dictyostelium discoideum*. J. Bone Miner. Res. **9**, 1029–1039
37 Eriksson, A. M., Zetterqvist, M. A., Lundgren, B., Andersson, K., Beije, B. and DePierre, J. W. (1991) Studies on the intracellular distributions of soluble epoxide hydrolase and of catalase by digitonin-permeabilization of hepatocytes isolated from control and clofibrate-treated mice. Eur. J. Biochem. **198**, 471–476
38 Schliebs, W. and Kunau, W. H. (2006) PTS2 co-receptors: diverse proteins with common features. Biochim. Biophys. Acta **1763**, 1605–1612
39 Nuttall, J. M., Motley, A. and Hettema, E. H. (2011) Peroxisome biogenesis: recent advances. Curr. Opin. Cell Biol. **23**, 421–426
40 Tsukamoto, T., Hata, S., Yokota, S., Miura, S., Fujiki, Y., Hijikata, M., Miyazawa, S., Hashimoto, T. and Osumi, T. (1994) Characterization of the signal peptide at the amino terminus of the rat peroxisomal 3-ketoacyl-CoA thiolase precursor. J. Biol. Chem. **269**, 6001–6010
41 Glover, J. R., Andrews, D. W., Subramani, S. and Rachubinski, R. A. (1994) Mutagenesis of the amino targeting signal of *Saccharomyces cerevisiae* 3-ketoacyl-CoA thiolase reveals conserved amino acids required for import into peroxisomes *in vivo*. J. Biol. Chem. **269**, 7558–7563
42 Froman, B. E., Edwards, P. C., Bursch, A. G. and Dehesh, K. (2000) ACX3, a novel medium-chain acyl-coenzyme A oxidase from *Arabidopsis*. Plant Physiol. **123**, 733–742
43 Hounslow, A. M., Carran, J., Brown, R. J., Rejman, D., Blackburn, G. M. and Watts, D. J. (2008) Determination of the microscopic equilibrium dissociation constants for risedronate and its analogues reveals two distinct roles for the nitrogen atom in nitrogen-containing bisphosphonate drugs. J. Med. Chem. **51**, 4170–4178
44 Palmieri, L., Rottensteiner, H., Girzalsky, W., Scarcia, P., Palmieri, F. and Erdmann, R. (2001) Identification and functional reconstitution of the yeast peroxisomal adenine nucleotide transporter. EMBO J. **20**, 5049–5059
45 van Roermund, C. W., Drissen, R., van Den Berg, M., Ijlst, L., Hettema, E. H., Tabak, H. F., Waterham, H. R. and Wanders, R. J. (2001) Identification of a peroxisomal ATP carrier required for medium-chain fatty acid β-oxidation and normal peroxisome proliferation in *Saccharomyces cerevisiae*. Mol. Cell. Biol. **21**, 4321–4329
46 Gupta, S. D., Mehan, R. S., Tansey, T. R., Chen, H. T., Goping, G., Goldberg, I. and Shechter, I. (1999) Differential binding of proteins to peroxisomes in rat hepatoma cells: unique association of enzymes involved in isoprenoid metabolism. J. Lipid Res. **40**, 1572–1584

47 Martin, D., Piulachs, M. D., Cunillera, N., Ferrer, A. and Belles, X. (2007) Mitochondrial targeting of farnesyl diphosphate synthase is a widespread phenomenon in eukaryotes. Biochim. Biophys. Acta **1773**, 419–426

48 Rogers, M. J., Xiong, X., Brown, R. J., Watts, D. J., Russell, R. G., Bayless, A. V. and Ebetino, F. H. (1995) Structure-activity relationships of new heterocycle-containing bisphosphonates as inhibitors of bone resorption and as inhibitors of growth of *Dictyostelium discoideum* amoebae. Mol. Pharmacol. **47**, 398–402

49 Bergstrom, J. D., Bostedor, R. G., Masarachia, P. J., Reszka, A. A. and Rodan, G. (2000) Alendronate is a specific, nanomolar inhibitor of farnesyl diphosphate synthase. Arch. Biochem. Biophys. **373**, 231–241

50 van Beek, E., Pieterman, E., Cohen, L., Lowik, C. and Papapoulos, S. (1999) Nitrogen-containing bisphosphonates inhibit isopentenyl pyrophosphate isomerase/farnesyl pyrophosphate synthase activity with relative potencies corresponding to their antiresorptive potencies *in vitro* and *in vivo*. Biochem. Biophys. Res. Commun. **255**, 491–494

Received 8 May 2012/13 July 2012; accepted 31 July 2012
Published as BJ Immediate Publication 31 July 2012, doi:10.1042/BJ20120750